Binding of Fatty Acids to β-Cryptogein: Quantitative Structure−Activity Relationships and Design of Selective Protein Mutants

Petr Dobeš,[†,‡] Jan Kmuníček,[†] Vladimír Mikeš,[‡] and Jiří Damborský*,[†]

National Centre for Biomolecular Research and Department of Biochemistry, Faculty of Science, Masaryk University, Kotlarska 2, 611 37 Brno, Czech Republic

Binding of fatty acids to cryptogein, the proteinaceous elicitor from Phytophthora, was studied by using molecular docking and quantitative structure−activity relationships analysis. Fatty acids bind to the groove located inside the cavity of cryptogein. The structure−activity model was constructed for the set of 27 different saturated and unsaturated fatty acids explaining 87% (81% cross-validated) of the quantitative variance in their binding affinity. The difference in binding between saturated and unsaturated fatty acids was described in the model by three electronic descriptors: the energy of the lowest unoccupied molecular orbital, the energy of the highest occupied molecular orbital, and the heat of formation. The presence of double bonds in the ligand generally resulted in stronger binding. The difference in binding within the group of saturated fatty acids was explained by two steric descriptors, i.e., ellipsoidal volume and inertia moment of length, and one hydrophobicity descriptor, i.e., lipophility. The developed model predicted strong binding for two biologically important molecules, geranylgeraniol and farnesol playing an important role in plant signaling as lipid anchors of some membrane proteins. Elicitin mutants selectively binding only one type of ligand were designed for future experimental studies.

INTRODUCTION

Study of relationships between a pathogen and a plant is important for protection of plants against infections. Elicitors are the molecules participating in the plant-pathogen interactions. Secretion of elicitors by a pathogen to the surrounding environment and their interaction with plant cells can induce plant hypersensitive reaction. Elicitins make up the highly conserved family of protein elicitors.[1] They are secreted specifically by the fungi *Oomycete* genera *Pythium* and *Phytophthora*.[2,3] The biological function of elicitins is currently unknown. The study of physiological effects on tobacco plants revealed that elicitins have the ability to induce so-called "systemic acquired resistance" against the pathogen attack accompanied by restricted leaf necrosis.[3,4] The response is induced by the interaction of elicitins with a putative receptor located on the cytoplasmic membrane of tobacco cells[5] composed of a calcium channel[6] and a glycoprotein.[7] The transfer of a signal through the receptor triggers phosphorylation-dephosphorylation cascades in the tobacco resulting in alkalinization of the extracellular medium, efflux of potassium and chloride ions, influx of calcium, production of the active species from oxygen,[5,8] and changes in the composition of the cell wall.[9] The primary structure of mature elicitins is composed of 98 amino acids (10 kDa) that are interconnected by three disulfide bridges. Elicitins can be classified according to their *pI* as α-elicitins (*pI* < 7) and β-elicitins (*pI* > 7). The β-elicitins generally induce a greater necrotic effect than the α-elicitins[10] due to

the presence of polar amino acids at necrotic sites located on the protein surface.[11,12]

The three-dimensional structures of two elicitin family members, cryptogein and cinnamomin, were determined by X-ray crystallography.[13,14] The structure of cryptogein was also studied by NMR spectroscopy.[15] The structures of elicitins are composed of five α-helices and one β-sheet arranged in a unique protein fold. A hydrophobic cavity is located in the protein core and connected with the protein surface by a tunnel. The original proposal that elicitins may facilitate transfer of sterols[16] was corroborated by the crystal structures of cryptogein in complex with dehydroergosterol (DHE)[17] and cholesterol.[18] Binding of ligands to the cavity seems to be essential for consecutive association of the elicitin with a receptor and induction of a biological response in a plant.[19] Besides sterols, also fatty acids (FAs) can bind to the internal cavity of elicitins[20] making them functionally similar to the family of plant lipid transfer proteins. Interestingly, plant lipid transfer proteins can associate with the same receptor in tobacco as elicitins,[21] and they can bind FAs and phospholipids but not sterols.

Here we study binding of FAs to the protein cryptogein at atomic detail. Models of the FA-crytogein complexes were constructed by molecular docking to obtain information about position and conformation of ligands inside the cavity. These models consequently served for design of mutant proteins binding selectively one type of ligand. The physicochemical properties important for the binding were identified by quantitative structure−activity relationships (QSAR) analysis, and the model served for prediction of binding affinities of two lipids, farnesol and geranylgeraniol, that play an important role in plant signaling.[22]

---

* Corresponding author e-mail: jiri@chemi.muni.cz.
† National Centre for Biomolecular Research.
‡ Department of Biochemistry.

METHODS

Modeling of Protein−Ligand Complexes. Protein−ligand complexes were constructed by the method of molecular docking using the program AUTODOCK 3.0.[23] The structure of protein cryptogein in the open state was obtained by withdrawal of DHE and water molecules from the crystal structure of the cryptogein-DHE complex solved to the resolution 2.15 Å (PDB-ID 1BXM). The open state corresponds to the structure with the first α-helix rearranged and with three side-chains of hydrophobic residues rotated outside the protein core thus creating a larger cavity for ligands. The hydrogen atoms were added by using the program WHATIF 5.0.[24] Energy maps were calculated by the AUTOGRID module of AUTODOCK with the size 100 × 100 × 100 points and separation 0.25 Å. The structures of ligands (Table 1) were created in the program INSIGHT II (Accelrys, U.S.A.), geometries were energetically optimized by the program MOPAC 6.0 (QCPE, U.S.A.), and rotatable bonds were assigned using the AUTOTORS module of AUTODOCK. The carboxyl group of FAs was modeled as ionized according to pH 7.0 and used for experimental determination of the binding constants.[20] Docking itself was conducted by Lamarckian genetic algorithm using the following parameters: 50 runs for every docking, 50 individuals in a population, the maximal degree of evaluation 1.5×10^6, the maximal number of generation 27 000, the value of elitism 1, the rate of mutation 0.02, and the rate of crossing-over 0.5. A local search was based on pseudo-Solis and Wets algorithm with the maximum of iterations 300. Resulting orientations from every docking run were divided into groups using cutoff root mean-squared deviation (RMSD) 0.5 Å.

Construction of QSAR Model. Molecular descriptors listed in Table 2 were calculated using the programs TSAR 3.1 and VAMP 6.0 (Accelrys, U.S.A.). The molecular structures were built in the program Insight II (Accelrys, U.S.A.), optimized in a vacuum using the AM1 method and the BFGS minimization algorithm and read to the spreadsheet of program TSAR. Alternatively, biologically relevant conformations were obtained from the molecular docking. TSAR calculates molecular descriptors, i.e., physicochemical properties, structural parameters, and topological indexes, in the batch mode using the algorithms described in the program manual. The quantum mechanical descriptors, i.e., energies of frontier molecular orbitals and dipole moments, were calculated using the semiempirical molecular orbital package VAMP interfaced by TSAR. AM1 Hamiltonian was used for these calculations. Partial Least Squares Projection to Latent Structures (PLS) was used for identification of variables important for an explanation of experimental data.[25] PLS is a multivariate projection method designed for extraction and visualization of hidden phenomena in the data by correlating principal components of an independent (X) and a dependent (Y) data matrix. In our case, the X matrix was represented by molecular descriptors and a y vector by experimentally determined binding affinity (Table 1). The data set used for development of the QSAR models reported in this study is available from the Internet at http://ncbr.chemi.muni.cz/∼jiri/resources.html#qsar. Variable selection was done manually based on the visual inspection of scores, loadings, and variable importance in projection plots.[26] The statistical quality of the models was evaluated
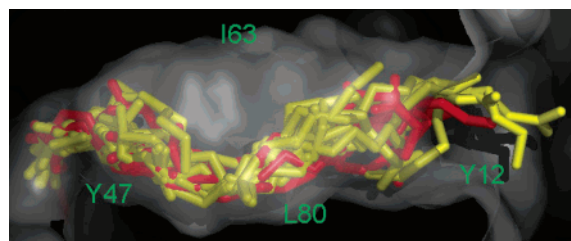

Figure 1. FA molecules docked to the cavity of cryptogein. Carbon chains align lengthwise with the groove located in the cavity. Saturated FAs (18 molecules) are in yellow, while unsaturated FAs (11 molecules) are in red. Active site is represented by the molecular surface with selected amino acids labeled. The hydrogen atoms are not shown for clarity.

by the correlation coefficient (R^2) and the cross-validated correlation coefficient (Q^2). The permutation test was conducted to access the risk of autocorrelation.

RESULTS

Molecular docking was used for the positioning of ligands to the internal cavity of cryptogein. Initially, the DHE molecule was removed from the cavity and docked back to the protein in order to optimize and validate the docking protocol. Docked orientation agreed well with the orientation from the crystal structure with RMSD equal to 1.4 Å. The hydrogen bond between DHE and Y47 was correctly identified by docking. All 29 FAs were docked to the cavity of cryptogein, and the quality of the fit was accessed by the scoring energies of the program AUTODOCK. The best orientations of the unsaturated FAs had the carbon chain positioned lengthwise of the groove located inside the protein cavity. Docking of long-chain saturated FAs provided two equally good orientations with ligand molecules bound in packed and extended conformation. The difference of the scoring energies between packed and extended conformation was negligible, but QSAR analysis revealed that only the extended conformation is biologically relevant. Furthermore, the similar binding mode for all studied ligands was obtained using extended conformations for long-chain saturated FAs (Figure 1) even though the superposition of the carboxylic group of all ligands could not be achieved due to the extreme length of some of the ligands compared to the size of the internal cavity of cryptogein. FAs bound to the cavity interact mainly with the residues making up the groove: Y33, P42, Y47, L41, V75, L80, L82, and Y87.

QSAR analysis was conducted for the data matrix of 29 ligands described by 28 molecular descriptors (X) and 1 experimentally determined binding affinity (y). Molecular descriptors calculated for the conformations of FAs obtained from the molecular docking, i.e., representing biologically relevant conformations, were used for the construction of QSAR models presented in the further text. Descriptors derived for the structures from docking were superior to the descriptors derived for the ground state conformations. This was confirmed by comparison of the statistical parameters of the QSAR models constructed for the two respective sets of descriptors (0.1 difference in R^2 and Q^2). The binding affinity describes the strength of ligand binding to the cryptogein and is defined as the ability of a ligand to displace DHE from the DHE-cryptogein complex. Briefly, the binding of DHE was measured as its fluorescence at 370 nm.
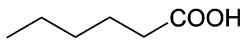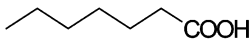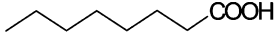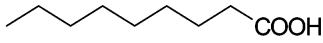
Table 1. List of Ligands
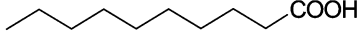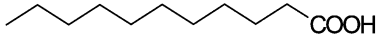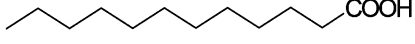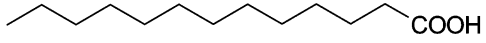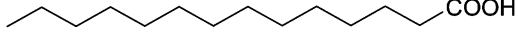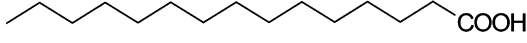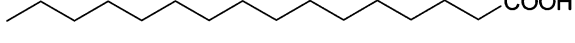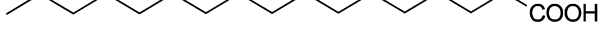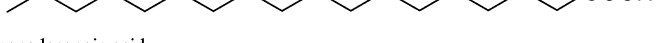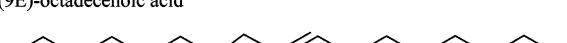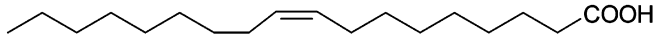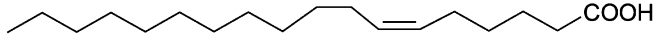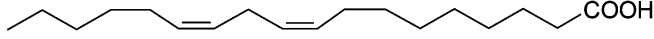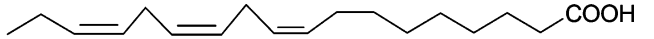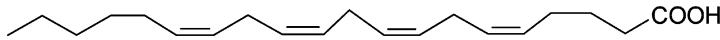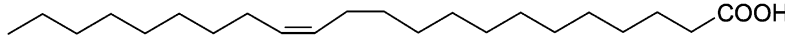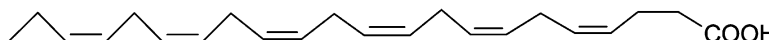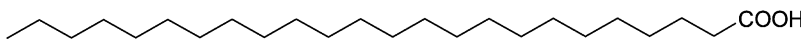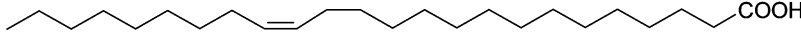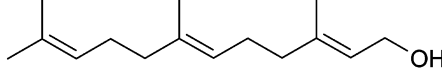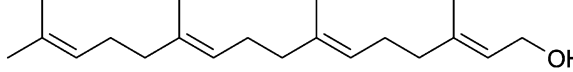
Systematic name and formula	Code	Bind. aff. [a]
hexanoic acid	m6s	91.2
heptanoic acid	m7s	73.6
octanoic acid	m8s	93.8
nonanoic acid	m9s	75.5
decanoic acid	m10s	70.7
undecanoic acid	m11s	75.5
dodecanoic acid	m12s	75.6
tridecanoic acid	m13s	64.7
tetradecanoic acid	m14s	93.8
pentadecanoic acid	m15s	83.9
hexadecanoic acid	m16s	99.1
heptadecanoic acid	m17s	92.4
octadecanoic acid	m18s	108.1
nonadecanoic acid	m19s	109.4
eicosanoic acid	m20s	111.5
heneicosanoic acid	m21s	106.3
docosanoic acid	m22s	104.3
triacosanoic acid	m23s	95.8
(9Z)-hexadecenoic acid	m16n9c	47.0
(9E)-octadecenoic acid	m18n9t	87.8

QSAR for Binding of Fatty Acids to Elicitin

J. Chem. Inf. Comput. Sci., Vol. 44, No. 6, 2004 **2129**

Table 1. List of Ligands

Systematic name and formula	Code	Bind. aff. [a]
(9Z)-octadecenoic acid	m18n9c	29.5
(6Z)-octadecenoic acid	m18n6c	60.1
(9Z,12Z)-octadecdienoic acid	m18n912c	16.7
(9Z,12Z,15Z)-octadectrienoic acid	m18n91215c	50.8
(5Z,8Z,11Z,14Z,)-eicostetraenoic acid	m20n581114c	34.6
(13Z)-docosenoic acid	m22n13c	58.5
(4Z,7Z,10Z,13Z,16Z,19Z)-docosahexenoic acid	m22n4710131619c	37.3
tetracosanoic acid	m24s	101.8
(15Z)-tetracosanoic acid	m24n15c	114.8
farnesol	far	26.0 [b]
geranylgeranyol	gerger	32.2 [b]

[a] Relative binding affinity of FAs to cryptogein. Data from ref 20. [b] Values predicted from the model M3.

Cryptogein (250 nM) and DHE (100 nM) were incubated together in a buffer, and fluorescence of the complex was recorded. Thereafter the FA (18 μM) was added. The binding affinity of a FA was expressed as a percentage of the fluorescence of the cryptogein-DHE complex and was inversely proportional to the fluorescence in the presence of FA (data adopted from publication[20]). The smaller value of fluorescence corresponds to the higher strength of FA binding to the cryptogein. The initial QSAR model (M1) was developed for all FAs and all descriptors (Table 3). This model showed moderate statistical quality but assisted in identification of two outliers: (9Z)-octadecenoic acid (m18n9c) and (9Z,12Z)-octadecdienic acid (m18n912c). These two molecules showed the strongest binding to the cryptogein in the experiment. However, experimental values did not correspond to the scoring energies obtained from the docking, which showed good correlation with binding affinity for all other molecules in the data set (not shown). Either m18n9c and m18n912c bind to the cavity by a different binding mode compared to other molecules or their binding affinities were overestimated in the experiment. The new QSAR model

(M2) has been derived for 27 FAs and 28 molecular descriptors. The large difference between R^2 and Q^2 indicates the presence of redundant variables, which were removed in the final (M3) model (Table 3). The final model shows good fit ($R^2 = 0.87$) and good internal predictive ability ($Q^2 = 0.81$). The model satisfactorily explains the difference in binding of saturated and unsaturated FAs (Figure 2). The variance between these two subgroups is described by the electronic parameters: the energy of the lowest unoccupied molecular orbital (LUMO), the energy of the highest occupied molecular orbital (HOMO), and the heat of formation (HF). We believe that energies of the frontier orbitals and heat of formation are not related to the binding process directly, but they capture different conformational behavior of FAs originating from the presence or absence of double bonds in their structures. The double bonds restrict the conformational freedom of unsaturated FAs compared to their saturated analogous and keep the molecules in the extended conformation needed for their binding to the internal cavity of elicitin (Figure 1). The remaining variance within the group of saturated FAs is explained by two steric

Table 2. List of Molecular Descriptors

code	descriptor	program
MM	molecular mass	TSAR 3.1
SA	size of molecular surface	TSAR 3.1
MV	size of molecular volume	TSAR 3.1
M1s	inertia moment 1−size	TSAR 3.1
M2s	inertia moment 2−size	TSAR 3.1
M3s	inertia moment 3−size	TSAR 3.1
M1l	inertia moment 1−length	TSAR 3.1
M2l	inertia moment 2−length	TSAR 3.1
M3l	inertia moment 3−length	TSAR 3.1
EV	size of ellipsoidal volume	TSAR 3.1
Log P	octanol−water partition coeff.	TSAR 3.1
LIP	lipophility	TSAR 3.1
LIPx	X lipophilic component	TSAR 3.1
LIPy	Y lipophilic component	TSAR 3.1
LIPz	Z lipophilic component	TSAR 3.1
MR	molecular refractivity	TSAR 3.1
TE	total energy	VAMP 6.0
EE	electronic energy	VAMP 6.0
NE	nuclear energy	VAMP 6.0
POL	mean polarizability	VAMP 6.0
HF	heat of formation	VAMP 6.0
LUMO	energy LUMO	VAMP 6.0
HOMO	energy HOMO	VAMP 6.0
DIPv	dipole moment	VAMP 6.0
DIPxv	X component dipole moment	VAMP 6.0
DIPyv	Y component dipole moment	VAMP 6.0
DIPzv	Z component dipole moment	VAMP 6.0

Table 3. List of QSAR Models

model	M1	M2	M3
number of objects (n)	29	27[a]	27[a]
number of descriptors (X)	28	28	6[b]
number of components (A)	2	2	3
correlation coeff. (R^2)	0.58	0.79	0.87
cross-validated correlation coeff. (Q^2)	0.34	0.68	0.81

[a] Excluded objects m18n9c and m18n912c. [b] Remaining variables M1l, EV, LIP, HF, LUMO, and HOMO.

and one hydrophobicity descriptor: ellipsoidal volume (EV), inertia moment of length (M1l), and lipophility (LIP), respectively.

Geranylgeranyol and farnesol resemble FAs in the length of nonbranched hydrophobic chain and in the terminal polar group. The QSAR model could be therefore used for the prediction of their binding affinity. Molecular descriptors were calculated for the structures in their docked conformations. The predicted values of relative binding affinity for farnesol and geranylgeranyol are 26.0 and 32.6, respectively.

DISCUSSION

Biological activity of elicitins is correlated with their ability to bind sterol.[19] It is probably the elicitin-sterol complex that binds to the receptor located on the cytoplasmatic membrane and induces a physiological response in tobacco. The sterol molecule bound inside the cavity may induce conformational changes necessary for the binding of elicitin to the receptor and triggering the plant defense reaction.[19] Cryptogein is a nonspecific sterol carrier protein able to bind sterols and FAs.[20] Unlike sterols, free FAs are not present in noticeable amounts in membranes but can be liberated by the action of phospholipases A_1 and A_2. Plant lipid transfer proteins (LTPs) are able to bind and transfer FAs and phospholipids but not sterols.[21] Among them, LTPs1 are constitutively expressed in specific tissues and/or induced as a response to stress. LTPs1 and elicitins share some structural and functional properties and compete with elicitins in binding to the same membrane receptors in tobacco.[27] The study of the other ligands that bind to the elicitins and LTPs and induce similar conformational changes as sterols is important for understanding of the elicitin-receptor interactions. The relationship between the complexation of elicitin with sterol and FA, respectively, is currently unknown and the design of protein mutants selectively binding either molecule can stimulate future research.

Computer modeling was used here to analyze complexation of elicitin β-cryptogein with FAs, geranylgeranyol, and farnesol, respectively. The binding mode of 29 different FAs, geranylgeranyol, and farnesol was predicted by using molecular docking. FAs bind to the groove located inside the
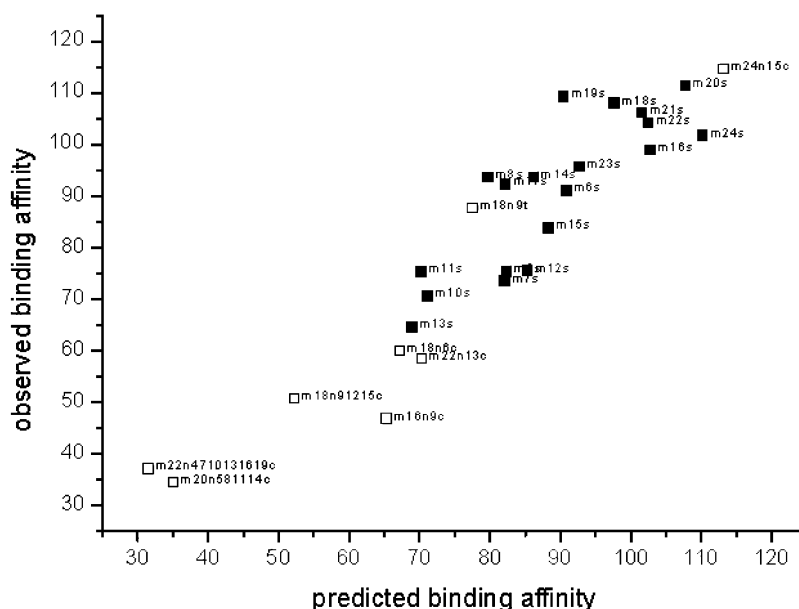

Figure 2. Plot of experimentally observed versus predicted binding affinities. Predictions were made using the QSAR model M3. Codes for FAs are provided in Table 1. Saturated FAs are represented by the filled squares, while unsaturated FAs are represented by empty squares.
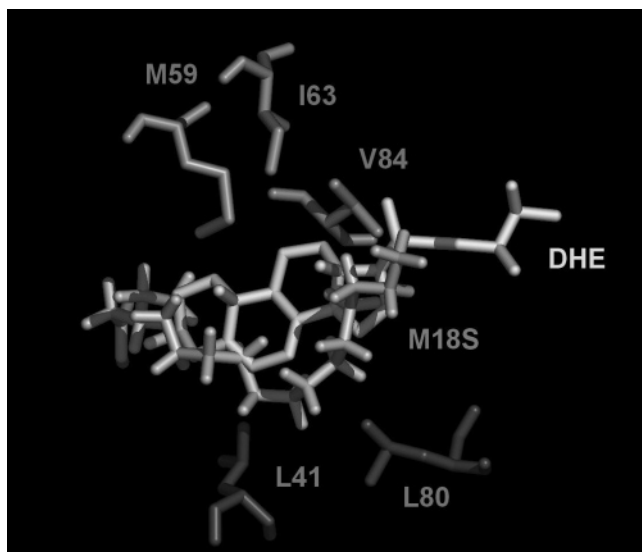
QSAR for Binding of Fatty Acids to Elicitin

J. Chem. Inf. Comput. Sci., Vol. 44, No. 6, 2004 **2131**

Figure 3. Amino acid residues suitable for substitutions leading to the protein variants with selective binding of DHE or FA. Substitutions of the residue M59, I63, and V84 by bulky hydrophobic amino acids will result in cryptogein preferentially binding FAs, while the same substitutions of the residues L41 and L80 will provide proteins preferring DHE. Octadecanoic acid (m18s) is displayed as the representative FA. Carboxylic group octadecanoic acid aligns with the alcoholic group of DHE.

protein cavity (Figure 1). Geranylgeranyol and farnesol are widespread in plant and animal cells in a form of prenylated proteins. These covalently attached lipids are recognized as being critically important for cellular signaling processes. Here we show that geranylgeranyol and farnesol bind to elicitins as efficiently as FAs. The importance of these interactions with elicitins or LTPs for the cell signaling should be tested. Geranylgeranyol and farnesol resemble FAs by their hydrophobic carbon chain as well as a terminally positioned polar group and can bind to the cryptogein by the same mode. QSAR analysis revealed that the binding of unsaturated ligands to the cavity of cryptogein is determined by their size and hydrophobicity. The strength of binding predicted for geranylgeranyol and farnesol from the QSAR model is in the same range as observed with the most strongly binding FAs. This finding may have important biological implications.

Structural alignment of the DHE-cryptogein and FA-cryptogein complexes revealed a different location of the ligands within the cavity (Figure 3). The higher flexibility of FAs allows them to accommodate the active site of cryptogein better than the more rigid DHE. We propose that FAs will not induce conformational changes in the protein structure, e.g. repositioning of the omega loop, observed in the DHE-cryptogein complex.[17] This may have important implications for in/ability of the FA-ergosterol complexes to induce systemic acquired resistance. Comparison of DHE-cryptogein and FA-cryptogein complexes enabled us to design of mutations favoring one type of ligand molecule only. Substitution of the residues M59, I63, or V84 by a large hydrophobic amino acid, e.g. phenylalanine or tryptophan, should reduce binding of sterol to the cavity of cryptogein. These mutations should not have an effect on the binding of FAs, farnesol, and geranylgeranyol, filling a free space next to the molecules bound in the groove. Substitution in the position I63 is the most suited for this

purpose, because it is located right to the groove of protein. Substitutions of the amino acid residues L41 and L80 for larger hydrophobic amino acids should distinctively decrease binding of FAs, farnesol, and geranylgeranyol in the groove of the cavity, while preserving the binding of sterol. Characterization of protein mutants showing selective binding is currently ongoing in our laboratory.

REFERENCES AND NOTES

(1) Huet, J. C.; Pernollet, J. C. Amino acid sequence of cinnamomin, a new member of the elicitin family, and its comparison to cryptogein and capsicein. *FEBS Lett.* **1989**, *257*, 302−306.

(2) Huet, J. C.; Lecaer, J. P.; Nespoulous, C.; Pernollet, J. C. The relationships between the toxicity and the primary and secondary structures of elicitin like protein elicitors secreted by the phytopathogenic fungus *Pythium Vexans. Mol. Plant-Microbe Interact.* **1995**, *8*, 302−310.

(3) Ricci, P.; Bonnet, P.; Huet, J. C.; Sallantin, M.; Beauvais-Cante, F.; Bruneteau, M.; Billard, V.; Michel, G.; Pernollet, J. C. Structure and activity of proteins from pathogenic fungi *Phytophthora* eliciting necrosis and acquired resistance in tobacco. *Eur. J. Biochem.* **1989**, *183*, 555−563.

(4) Kamoun, S.; Klucher, K. M.; Coffey, M. D.; Tyler, B. M. A gene encoding a host-specific elicitor protein of *Phytophthora parasitica. Mol. Plant-Microbe Interact.* **1993**, *6*, 573−581.

(5) Blein, J. P.; Milat, M. L.; Ricci, P. Responses of cultured tobacco cells to cryptogein, a proteinaceous elicitor from *Phytophthora cryptogea*—possible plasmalemma involvement. *Plant Physiol.* **1991**, *95*, 486-491.

(6) Pineiros, M.; Tester, M. Charakterization of a voltage-dependent Ca2++-selective channel from wheat. *Planta* **1995**, *195*, 478−488.

(7) Bourque, S.; Binet, M. N.; Ponchet, M.; Pugin, A.; Lebrun-Garcia, A. Characterization of the cryptogein binding sites on plant plasma membranes. *J. Biol. Chem.* **1999**, *274*, 34699−34705.

(8) Rusterucci, C.; Stallaert, V.; Milat, M. L.; Pugin, A.; Ricci, P.; Blein, J. P. Relationship between active oxygen species, lipid peroxidation, necrosis, and phytoalexin production induced by elicitins in *Nicotiana. Plant Physiol.* **1996**, *111*, 885−891.

(9) Kieffer, F.; Lherminier, J.; Simon-Plas, F.; Nicole, M.; Paynot, M.; Elmayan, T.; Blein, J. P. The fungal elicitor cryptogein induces cell wall modifications on tobacco cell suspension. *J. Exp. Bot.* **2000**, *51*, 1799−1811.

(10) Nespoulous, C.; Huet, J. C.; Pernollet, J. C. Structure−function-relationships of alpha-elicitin and beta-elicitin, signal proteins involved in the plant-phytophthora interaction. *Planta* **1992**, *186*, 551−557.

(11) Panabieres, F.; Marais, A.; Le Berre, J. Y.; Penot, I.; Fournier, D.; Ricci, P. Characterization of a gene cluster of *Phytophthora cryptogea* which codes for elicitins, proteins inducing a hypersensitive-like response in tobacco. *Mol. Plant-Microbe Interact.* **1995**, *8*, 996−1003.

(12) Perez, V.; Huet, J. C.; O'Donohue, M.; Nespoulous, C.; Pernollet, J. C. A novel elicitin necrotic site revealed by alpha-cinnamomin sequence and site-directed mutagenesis. *Phytochemistry* **1999**, *50*, 961−966.

(13) Boissy, G.; de La Fortelle, E.; Kahn, R.; Huet, J. C.; Bricogne, G.; Pernollet, J. C.; Brunie, S. Crystal structure of a fungal elicitor secreted by *Phytophthora cryptogea*, a member of a novel class of plant necrotic proteins. *Structure* **1996**, *4*, 1429−1439.

(14) Rodrigues, M. L.; Archer, M.; Martel, P.; Jacquet, A.; Cravador, A.; Carrondo, M. A. Structure of beta-cinnamomin, a protein toxic to some plant species. *Acta Crystallogr., Sect. D: Biol. Crystallogr.* **2002**, *58*, 1314−1321.

(15) Gooley, P. R.; Keizer, D. W.; Gayler, K. R.; Grant, B. R. The solution structure of beta-cryptogein by NMR spectroscopy. *Plant Physiol.* **1997**, *114*, 1138−1138.

(16) Mikes, V.; Milat, M. L.; Ponchet, M.; Ricci, P.; Blein, J. P. The fungal elicitor cryptogein is a sterol carrier protein. *FEBS Lett.* **1997**, *416*, 190−192.

(17) Boissy, G.; O'Donohue, M.; Gaudemer, O.; Perez, V.; Pernollet, J. C.; Brunie, S. The 2.1 A structure of an elicitin-ergosterol complex: a recent addition to the sterol carrier protein family. *Protein Sci.* **1999**, *8*, 1191−1199.

(18) Lascombe, M. B.; Ponchet, M.; Venard, P.; Milat, M. L.; Blein, J. P.; Prange, T. The 1.45 A resolution structure of the cryptogein-cholesterol complex: a close-up view of a sterol carrier protein (SCP) active site. *Acta Crystallogr., Sect. D: Biol. Crystallogr.* **2002**, *58*, 1442–1447.

(19) Osman, H.; Vauthrin, S.; Mikes, V.; Milat, M. L.; Panabieres, F.; Marais, A.; Brunie, S.; Maume, B.; Ponchet, M.; Blein, J. P. Mediation of elicitin activity on tobacco is assumed by elicitin-sterol complexes. *Mol. Biol. Cell* **2001**, *12*, 2825–2834.

(20) Osman, H.; Mikes, V.; Milat, M. L.; Ponchet, M.; Marion, D.; Prange, T.; Maume, B. F.; Vauthrin, S.; Blein, J. P. Fatty acids bind to the fungal elicitor cryptogein and compete with sterols. *FEBS Lett.* **2001**, *489*, 55–58.

(21) Blein, J. P.; Coutos-Thevenot, P.; Marion, D.; Ponchet, M. From elicitins to lipid-transfer proteins: a new insight in cell signaling involved in plant defence mechanisms. *Trends Plant Sci.* **2002**, *7*, 293–296.

(22) Thompson, G. A.; Okuyama, H. Lipid-linked proteins of plants. *Prog. Lipid Res.* **2000**, *39*, 19–39.

(23) Morris, G. M.; Goodsell, D. S.; Halliday, R. S.; Huey, R.; Hart, W. E.; Belew, R. K.; Olson, A. J. Automated docking using a Lamarckian genetic algorithm and an empirical binding free energy function. *J. Comput. Chem.* **1998**, *19*, 1639–1662.

(24) Vriend, G. WHAT IF: A molecular modeling and drug design program. *J. Mol. Graphics* **1990**, *8*, 52–56.

(25) Wold, S.; Johansson, E.; Cocchi, M. PLS–Partial Least-Squares Projections to Latent Structure*s*. In *3D QSAR in Drug Design: Theory, Methods and Application*; Kubynyi, H., Ed.; ESCOM: Leiden, 1993; pp 523–550.

(26) Eriksson, L.; Johansson, E.; Wold, S. Quantitative structure–activity relationship model validation. In *Quantitative Structure–Activity Relationships in Environmental Sciences – VII*; Chen, F., Schüürmann, G., Eds.; SETAC Press: Pensacola, 1997; pp 5–20.

(27) Buhot, N.; Douliez, J. P.; Jacquemard, A.; Marion, D.; Tran, V.; Maume, B. F.; Milat, M. L.; Ponchet, M.; Mikes, V.; Kader, J. C.; Blein, J. P. A lipid transfer protein binds to a receptor involved in the control of plant defence responses. *FEBS Lett.* **2001**, *509*, 27–30.